Molecular Catalysis 484 (2020) 110774

Contents lists available at ScienceDirect

Molecular Catalysis

journal homepage: www.elsevier.com/locate/mcat

# Mechanistic perspectives on piperidine-catalyzed synthesis of 1,5-benzodiazepin-2-ones

Hanaa Mansour[a], Morad M. El-Hendawy[b,*]

[a] Department of Chemistry, Faculty of Science, Kafrelsheikh University, Kafrelsheikh 33516, Egypt
[b] Department of Chemistry, Faculty of Science, New Valley University, Kharga 72511, Egypt

ARTICLE INFO

*Keywords:*
1,5-Benzodiazepin-2-one
Organocatalyst
Ethanol-assisted mechanism
Density functional calculations

ABSTRACT

This work introduced new members to the pharmaceutical family of 1,5-benzodiazepin-2-ones, $\mathbf{2_{a-e}}$. These compounds were synthesized in moderate yields *via* the reaction of 1,2-bifunctional substrates (α-cyanocinnamates) with *o*-phenylenediamine in xylene. The conduction of the above reaction in the presence of piperidine has produced amazing product, *N*-alkenylimidazolone derivative **(5)**, in addition to the traditional one, 1,5-benzodiazepin-2-one **($\mathbf{2_a}$)** in 3:1 ratio. The density functional theory (DFT) could successfully explain the role of piperidine as an organic catalyst to produce both products in this ratio through ethanol-assisted mechanisms. It is also amazing that we could obtain **5** solely by the dry fusion of $\mathbf{2_a}$ through the thermal contraction of diazepinone ring into imidazolone one. The mechanism of diazepinone-imidazolone transformation was proposed and validated by the DFT calculations. The findings showed that the precise proton transfer of primary amino hydrogen of $\mathbf{2_a}$ is the play-maker in the reaction game. The proposed mechanisms of the three transformations can be useful for investigation of the formation and deformation of other 1,5-diazepine systems.

## 1. Introduction

Design of privileged structures having valuable pharmacological benefits such as 1,5-benzodiazepin-2-ones is a targeted strategy in medicinal chemistry because they have a broad range of treatments such as analgesic, anti-aggressive, psychotropic, anticonvulsive, and anti-proliferative activities [1–7]. Fig. 1 shows some commercial drugs based on 1,5-benzodiazepin-2-one scaffold include lofendazam, arfendazam, and clobazam [5]. It is evident that there is an increasing need in medicinal chemistry to introduce new scaffolds [3,8–19]; thus, our goal herein was the addition of new members to this family.

Methods for the synthesis of benzodiazepines were formed mainly *via* coupling of *o*-phenylenediamine (**OPD**) with a variety of ketones [20] and chalcones [21], alkynes and other precursors [22–25]. The use of an inexpensive substrate with a simple catalytic system for synthesis of new members of benzodiazepine-based family with the formation of multiple bonds (C–C/C=N/C–N), remains a highly desirable and continuous goal in current organic synthesis [26,27]. Recently great efforts have been made to develop new members in the 1,5-benzodiazepin-2-one family [28–35]. For instance, copper-catalyzed arylation of 2-azetidinone with 2-iodoaniline followed by transamidation promoted by 50 mol% Ti(OiPr)4 in toluene at 110 °C provided 1,5-benzodiazepin-2-one in excellent yield [28]. Also, the reaction of **OPD** with spiroepoxy lactone within EtOH at reflux provided the 1,5-benzodiazepin-2-one after amide formation, mediated by t-BuMgBr [29]. The most used procedure for the synthesis of 1,5-benzodiazepin-2-ones was conducted by condensation of **OPD** with β-ketoesters [30,29–35]. The presence of an active methylene segment played an essential role in the mechanism. The novelty of the present work is the conduction of piperidine-catalyzed synthesis *via* coupling of **OPD** with the 1,2-bifunctional substrate (α-cyanocinnamate), *i.e.*, with the absence of active methylene segment. On the other hand, we proposed reaction mechanisms to explain these transformations, and the DFT method examined their validity.

## 2. Results and discussions

### 2.1. Synthesis and characterization

According to the pathway shown in Scheme 1, a stepwise synthesis of 1,5-benzodiazepin-2-ones $\mathbf{2_{a-e}}$ was carried out under simple reaction conditions (Scheme 1). Firstly, and according to Knoevenagel procedure [36], α-ethylcyanocinnamate derivatives ($\mathbf{1_{a-e}}$) were synthesized from the condensation of ethylcyanoacetate and various aldehydes in ethanol with addition of few drops of piperidine at 0 °C. Subsequently, $\mathbf{2_{a-e}}$ was successfully synthesized from mixing a molar ratio of **1** and **OPD** in xylene. The mixture was refluxed with stirring for

* Corresponding author.
*E-mail address:* morad.elhendawy@scinv.au.edu.eg (M.M. El-Hendawy).

https://doi.org/10.1016/j.mcat.2020.110774
Received 26 September 2019; Received in revised form 5 January 2020; Accepted 12 January 2020

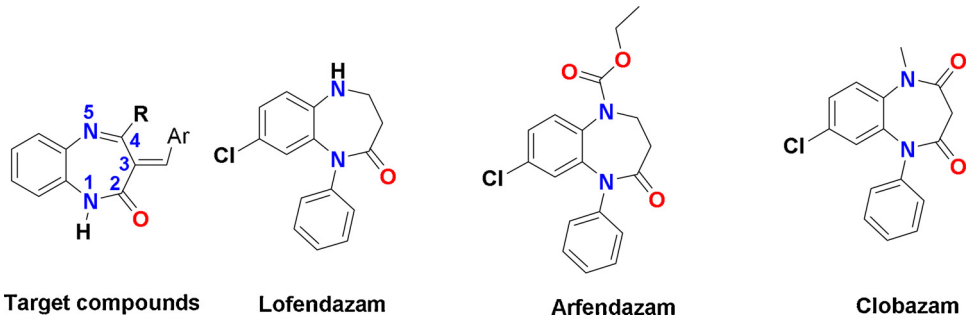


**Fig. 1.** Some commercial drugs based on a 1,5 – benzodiazepin – 2 – one scaffold [1,2, 4 – 7].

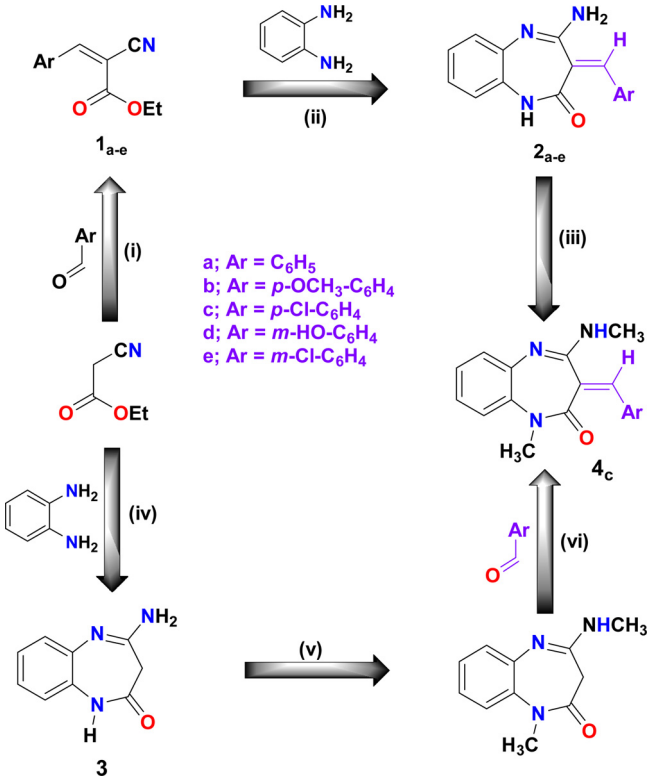


**Scheme 1.** Synthesis of the benzodiazepinones $\mathbf{2_{a-e}}$: (i) EtOH / piperidine at 0 °C; (ii) xylene / reflux; (iii) methyl iodide; (iv) xylene / reflux; (v) methyl iodide, (vi) glacial acetic acid.

different times (see experimental part), which led to the formation of colorless to brown materials on cooling with about 50 % yield. Different spectroscopic techniques, such as IR, $^1$H NMR, $^{13}$C NMR, and mass spectrometry, were used to confirm the formation of $\mathbf{2_{a-e}}$; see the supporting information. The comparison of mass spectra of the products with those of the reactants confirms the elimination of only one ethanol molecule. IR absorption spectra of the enaminone group show a broad band around 3426 cm$^{-1}$ assigned for the NH groups. Also, the absence of the stretching frequency of cyano groups refers to the addition to that group. Characteristic bands were observed in the range of 1610 – 1627 cm$^{-1}$, which may be assigned for the (NH–CO–C=C) enaminone group [37]. Furthermore, the presence of the enaminone group in the products has been also proved by the decolorization of bromine in chloroform. $^1$H NMR spectra of $\mathbf{2_{a-e}}$ exhibit broad bands around δ = 6.50 ppm (exchanged by $D_2O$) for three protons, which further confirm the presence of NH and $NH_2$ groups.

To further prove the structures of 1,5-benzodiazepin-2-ones, $\mathbf{2_{a-e}}$, a different route has been conducted, as shown in Scheme 1. The first step is the formation of **3** from the reaction of ethylcyanoacetate and **OPD** in xylene with the elimination of one ethanol molecule as confirmed by mass spectra and elemental analysis. IR absorption band of the cyano group disappeared in the spectrum of **3,** and instead, new bands appeared around 3400 and 1590 cm$^{-1}$, which assigned for stretching vibration of the amino and > C=N groups, respectively. This could indicate the addition reaction at the cyano group. The characteristic bands at 1660 cm$^{-1}$ assigned for stretching vibration of the amide carbonyl group, which confirm the intramolecular cyclization reaction. $^1$H NMR spectrum of **3** exhibits a multiplet band around δ = 2.35 ppm corresponding to the $CH_2$ protons. The $NH_2$ and NH protons were observed at δ = 7.63 – 7.64 and 12.73 – 12.75 ppm (exchanged by $D_2O$), respectively. The characteristic aromatic protons were observed in the region of δ = 7.22 – 7.61 ppm. *N* – methylation of **3** using methyl iodide, followed by subsequent condensation with the *p*-chlorobenzaldehyde in glacial acetic acid under boiling conditions, produced the products, 1,5 – benzodiazapin – 2 – ones ($\mathbf{4_a}$), Scheme 1. A comparison of this material with that obtained *via* methylation of 1,5-benzodiazepin-2-ones $\mathbf{2_c}$ using methyl iodide showed identity by all criteria evaluated. $^1$H and $^{13}$C NMR spectra of the methylated product, $\mathbf{4_c}$, showed that both the primary and secondary amine nitrogen atoms had been methylated. The $NHCH_3$ and $NCH_3$ bands in $\mathbf{4_c}$ are coming at 3.80 and 3.85 ppm in the $^1$H NMR spectrum and 31.5 and 33.4 ppm in the $^{13}$C NMR spectrum, respectively.

Amazing product, *N*–alkenylbenzimidazolone **(5)** in addition to the expected product, 1,5-benzodiazepin-2-one derivative $\mathbf{(2_a)}$ were obtained by 1:3 ratio as a result to the piperidine-catalyzed reaction of $\mathbf{1_a}$ and **OPD**, Scheme 2. It is worth mentioning that Kumar and Kapoor have reported that this reaction under thermal conditions yielded ethyl 2 – cyano-3 – phenyl – propionoate, 2 – phenyl benzimidazole, and ethyl cyanoacetate without production of benzodiazepinone [38].

Interestingly, compound **5** was successfully prepared solely by either of dry fusion (45 % yield) of the $\mathbf{2_a}$ or the reaction of $\mathbf{1_a}$ with **OPD** in dilute hydrochloric acid (55 % yield), see Scheme 2 & Table 1. $FD^+$

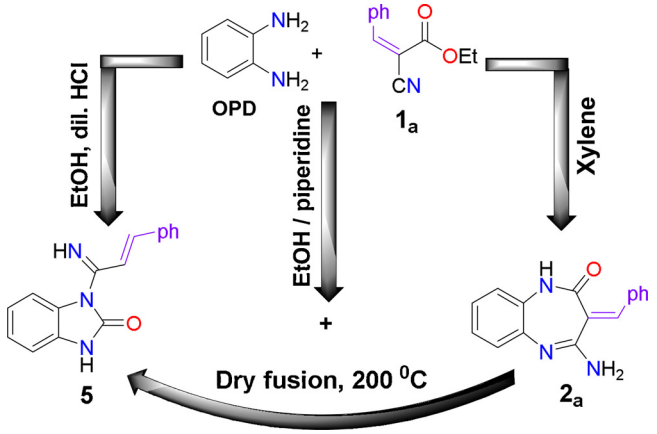


**Scheme 2.** Synthesis of *N*–alkenylbenzimidazolone **5** *via* different conditions; i) xylene; ii) EtOH / piperidine; iii) EtOH, dil. HCl; iv) dry fusion, 200 °C.

**Table 1**
Reaction conditions optimization.

|  | + |  | Solvent | Catalyst | Temp. | 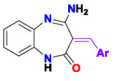 | 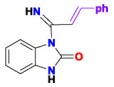 |
|---|---|---|---|---|---|---|---|
| | | Ar = ph | xylene | – | reflux | 50 % | – |
| | | Ar = *p*–$OCH_3$–ph | xylene | – | reflux | 59 % | – |
| | | Ar = *p*–Cl–ph | xylene | – | reflux | 51 % | – |
| | | Ar = *m*–HO–ph | xylene | – | reflux | 52 % | – |
| | | Ar = *m*–Cl–ph | xylene | – | reflux | 50 % | – |
| | | Ar = ph | EtOH | piperidine | r.t. | 40 % | 35 % |
| | | Ar = ph | EtOH | HCl | r.t. | – | 55 % |
| | | Ar = ph | – | – | | dry fusion[a] | 45 % |

[a] Dry fusion of the 1,5-benzodiazepin-2-one.

mass (THF) of **5** exhibited peak at $m/e = 263$ corresponding to the molecular ions peaks, $[\mathbf{5}]^+$. An IR broad band at 1920 and 840 $cm^{-1}$ assigned for NH═C−C═C fragment, while the NH group appears at 3400 $cm^{-1}$. A characteristic band at 1627 $cm^{-1}$ assigned for the imide carbonyl (NHC═O) group. Moreover, the $^1$H NMR spectrum of **5** is characterized by the appearance of a broad band at $\delta = 6.41 - 6.61$ ppm that corresponds to the three protons of NH and $NH_2$ (exchanged by $D_2O$). The α-styryl moiety was indicated by the appearance of two vinyl proton signals, *cis,* and *trans* to the phenyl ring, at $\delta = 5.50$ and 5.81 ppm [39]. The mechanism of diazepinone-imidazolone conversion, shown in Scheme 2, was studied deeply by the DFT method, as shown in the following section.

In order to study the reaction mechanisms and provide an explanation for the different outcomes of the transformations shown in Scheme 2, DFT calculations have been carried out. Ethanol, as a polar solvent, should play an essential role in stabilization of different intermediates and transition states species, especially in the case of proton transfer steps [40]. Thus, explicit consideration of one ethanol molecule was involved in the modeling to simulate experimental conditions. For simplicity, the ethanol molecules are not shown in Schemes 3 & 4 . The intermediates and transition states are denoted as $\mathbf{Int_n}$ and $\mathbf{TS_{n1\text{-}n2}}$, respectively, where **n1 and n2** refer to the initial and final intermediates around the transition state, respectively. The Cartesian coordinates of the optimized transition states located along the reaction coordinate for ethanol-assisted and thermal contraction mechanisms are shown in the Supporting information.

### 2.2. Computational mechanistic investigations

#### 2.2.1. The first transformation: a piperidine-catalyzed synthesis of 1,5-benzodiazepin-2-one, $2_a$

The proposed mechanism for the piperidine-catalyzed synthesis of $\mathbf{2_a}$ in EtOH is presented in Scheme 3, and its free energy profile is shown in Fig. 2. The reaction initiates by a fast step (6.09 kcal/mol), *i.e.*, nucleophilic addition of the secondary amine (piperidine) to the carbonyl group of $\mathbf{1_a}$ to form stable carbinolamine intermediate, $\mathbf{Int_1}$. Formation of new $C–N_{PIP}$ bond between $\mathbf{1_a}$ and **PPR** is coupled with proton transfer from the later to the former with the assist of one ethanol molecule, as shown in Fig. 2. The next step is slightly endergonic by 0.48 kcal/mol, where the ethoxy group leaves the $\mathbf{Int_1}$ to afford $\mathbf{Int_2}$ and one ethanol molecule through $\mathbf{TS_{1\text{-}2}}$ with an activation barrier 16.02 kcal/mol. In this context, $C–O_{EtOH}$ single bond broke with intramolecular proton transfer from hydroxyl oxygen to the ethoxy oxygen atom. $\mathbf{Int_2}$ is essential species because it defines the direction of the reaction. It possesses two active groups, > C═O, −C≡N; thus, the addition of **OPD** could occur on the electrophilic carbon of both of them to afford both $\mathbf{2_a}$ and **5** in the reaction mixture by ratio 1: 3, respectively, Schemes 3 & 4 . The carbon center of a nitrile is electrophilic;

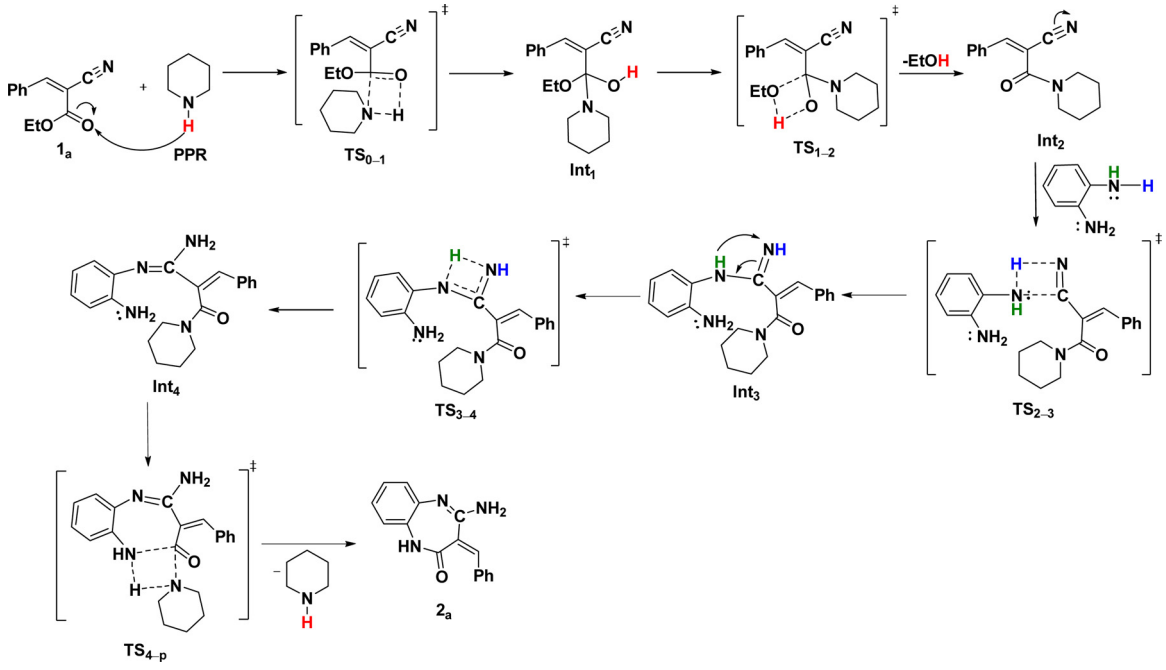


**Scheme 3.** Proposed mechanism for the piperidine-catalyzed synthesis of 1,5 − benzodiazepin-2 − one, $\mathbf{2_a}$, in EtOH.

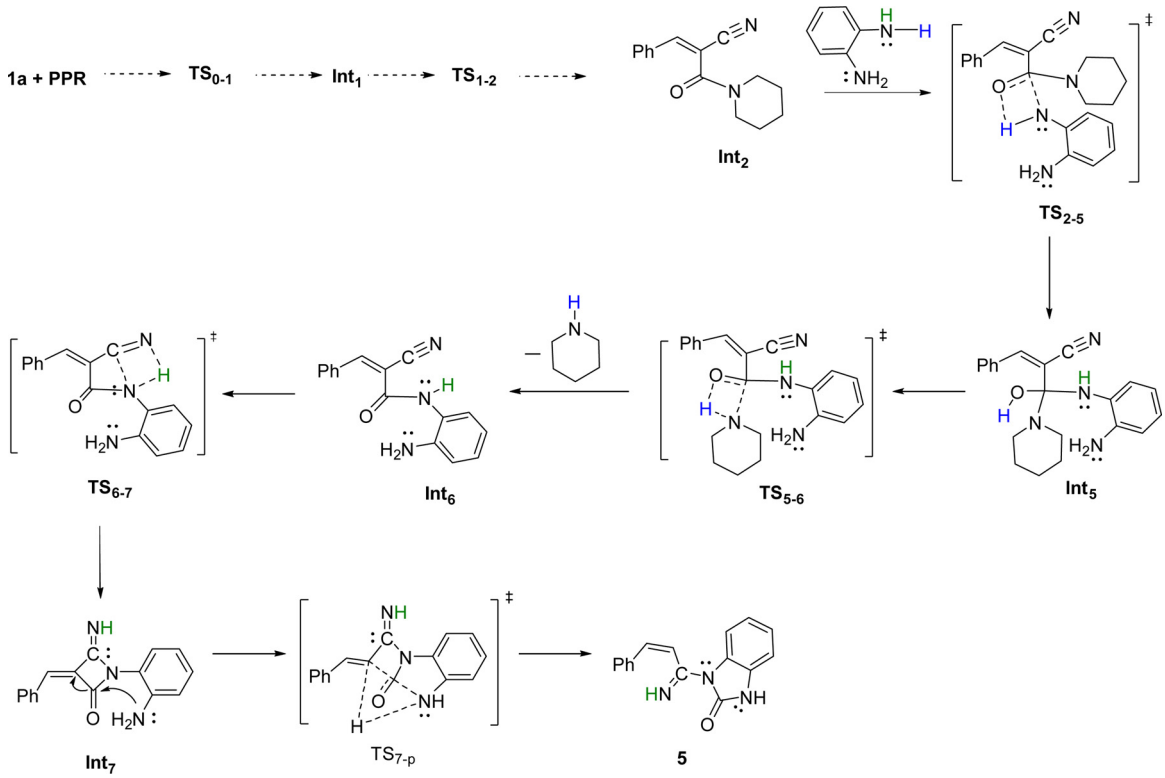


**Scheme 4.** The proposed mechanism for the piperidine – catalyzed the synthesis of *N*–alkenylbenzimidazolone, 5, in EtOH. The structures from reactants until $TS_{1-2}$ are shown in Scheme 3.

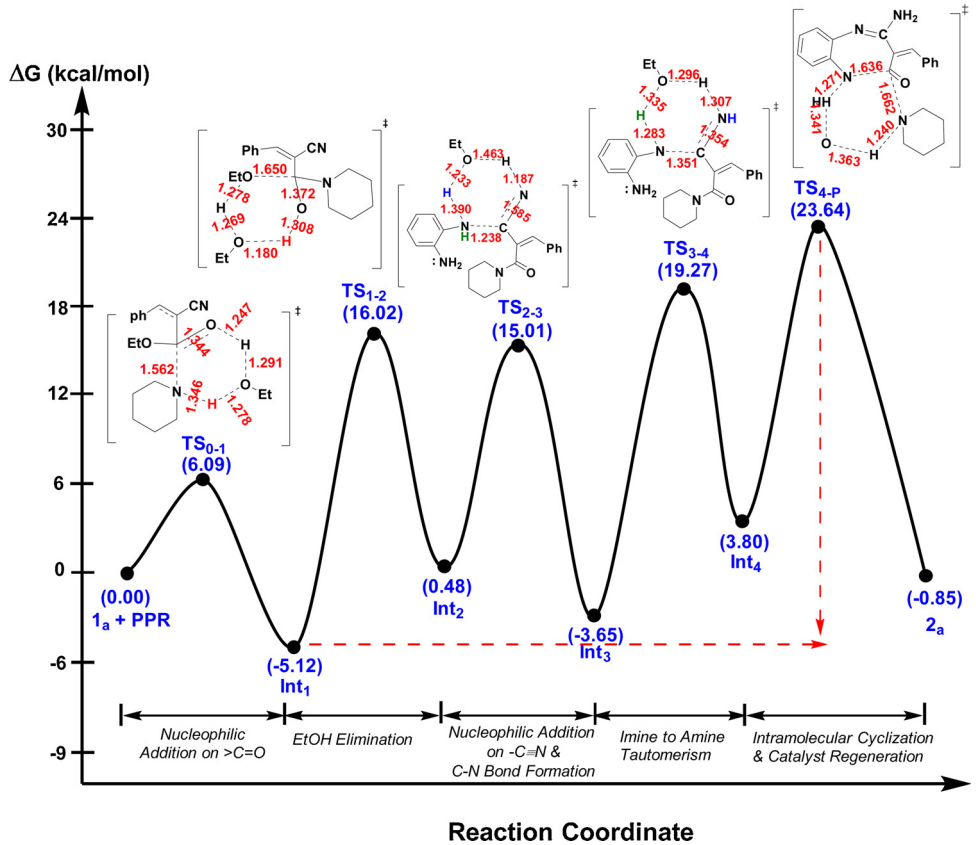


**Fig. 2.** Free energy profile of the piperidine-catalyzed synthesis of 1,5-benzodiazepin-2-one, $\mathbf{2}_a$, in EtOH. The red dashed line shows the overall activation barrier. (For interpretation of the references to colour in this figure legend, the reader is referred to the web version of this article.)

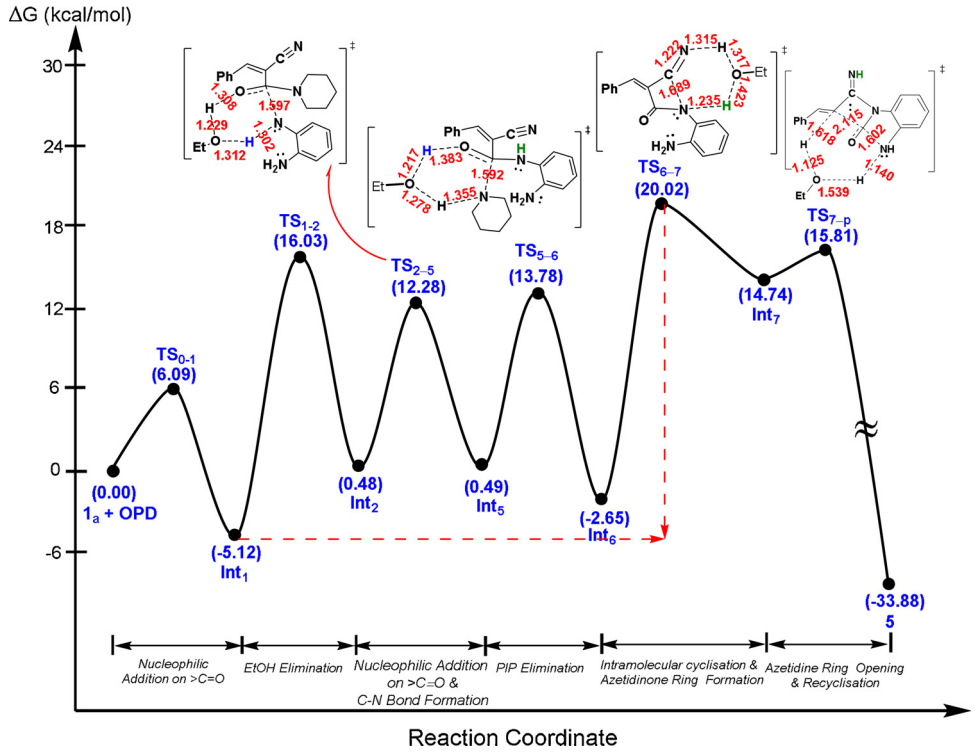


**Fig. 3.** Free energy profile of the piperidine-catalyzed synthesis of *N*-alkenylimidazolone derivative, **5**, in EtOH.

hence it is susceptible to the nucleophilic addition of the amino group of **OPD**. According to the calculations, the addition of **OPD** to the nitrile group represents a concerted process where the formation of C—$N_{OPD}$ bond and proton transfer occurred in one step. This step requires activation energy of 15.01 kcal/mol to produce exergonic intermediate, **$Int_3$**, by 3.65 kcal/mol. The fourth step is imine-amine tautomerism that affords an endergonic species with an energy barrier of 19.27 kcal/mol. The elimination of piperidine (**$TS_{4-p}$** in Fig. 2) is the rate-limiting step with an overall free energy barrier of 28.76 kcal/mol to afford the final product, **$2_a$,** which is staying only 0.85 Kcal/mol above the initial reactants.

### 2.2.2. The second transformation: a piperidine-catalyzed synthesis of N-alkenylimidazolone (5)

On the other hand, the **$Int_2$** interacts with **OPD** differently where the amino group of the later acts as a nucleophilic center to attack the electrophilic carbon of carbonyl group in the **$Int_2$** to produce an isoenergetic intermediate, **$Int_5$**. In such a case, the formation of a new C—N bond between **OPD** and **$Int_2$** is coupled with proton transfer from the less electropositive N-atom toward the electronegative O-atom of **$Int_2$** formed through **$TS_{2-5}$** with free energy barrier 12.28. It is evident that the activation barrier of **$Int_2$**→**$Int_5$** is more kinetically favorable than that of **$Int_2$**→**$Int_3$**, by *ca.* 3 kcal/mol, see Figs. 2 & 3 . This could explain the simultaneous attack of **OPD** on the nitrile and carbonyl carbon of **$Int_2$**, with the preferable production of the former.

The next step is the elimination of piperidine from **$Int_5$** to regenerate carbonyl group again in **$Int_6$**. To eliminate piperidine from **$Int_5$**, 13.78 kcal/mol is needed to break the C—N bond and to transfer proton from the hydroxyl group to the piperidine nitrogen. The cyclization step leading to 2-azetidinone ring formation, **$Int_7$**, is a rate-determining step for this reaction with an overall energy barrier of 25.14 kcal/mol. The formation of high endergonic **$Int_7$** (14.47 kcal/mol) occurred in a concerted step as a result of concurrent proton transfer from the secondary amine nitrogen to the imine nitrogen with C—$N_{OPD}$ bond formation. The reaction ended by intramolecular nucleophilic substitution, $S_N2$, where the free primary amine attack the exocyclic carbonyl group to form a new C—$N_{OPD}$ bond to break C—$C_{OPD}$ bond leading to imidazolone ring. In other words, the lifetime of the high energetic species, **$Int_7$**, is short because of the strain effect from the four-membered ring. Thus, the ring-opening of the azetidinone ring is an easy task for the sake of the formation of less strain five-membered ring. This molecular adaptation could be explained by the low activation energy of 15.81 kcal/mol to furnish the externally exergonic product, **5**, by 33.88 kcal/mol. The rate associated with this process is expected to be much higher than that leading to **$2_a$**, where the formation of **5** is 3.62 kcal/mol more favorable than that of **$2_a$** see Figs. 2 & 3 . After all, according to DFT findings, it can be stated that the formation of **$2_a$** and **5** can co-occur with the kinetic and thermodynamic preferable formation of the later as the main product, in accord with the experimental results.

### 2.2.3. The third transformation: thermal ring contraction of the benzodiazepinones $2_a$

The proposed mechanism to account for the formation of *N* − alkenylimidazolone **5** *via* thermal ring contraction of the benzodiazepinones **$2_a$** is depicted in Scheme 5. The calculations were performed in the gas phase to simulate the dry fusion experimental condition. The detailed theoretical analysis (Fig. 4) showed that the thermal ring contraction reaction could be described as a sequential three-step process. The initial step is the proton mediated amine/imine tautomerization of **$2_a$** into **$Int_8$** that is exergonic by 2.52 kcal/mol). As **$2_a$** moves to **$Int_8$**, significant structural changes occur through a four-membered ring transition state, **$TS_{2-8}$**, where $N_1$—$H_1$ and $N_3$—$H_1$ bonds are elongated to 1.355 and 1.376 Å, respectively with a high activation barrier, 20.56 kcal/mol. The formation of **$Int_8$** is followed by the intramolecular nucleophilic addition of the secondary amine (—$N_1H_1$—) on the carbonyl group (> $C_9$=$O_1$) to afford a highly endergonic species, diazabicyclo[3.2.0]heptanol, **$Int_9$**, *i.e.*, 14.86 kcal/mol higher than **$2_a$**. In this step, the diazepine ring split into the bicyclic ring, where a new $C_1$—$N_9$ bond is formed and proton transferred from the secondary amine hydrogen into the carbonyl oxygen. The final step is the intramolecular nucleophilic substitution, $S_N2$, on the exocyclic $C_8$=$C_{10}$

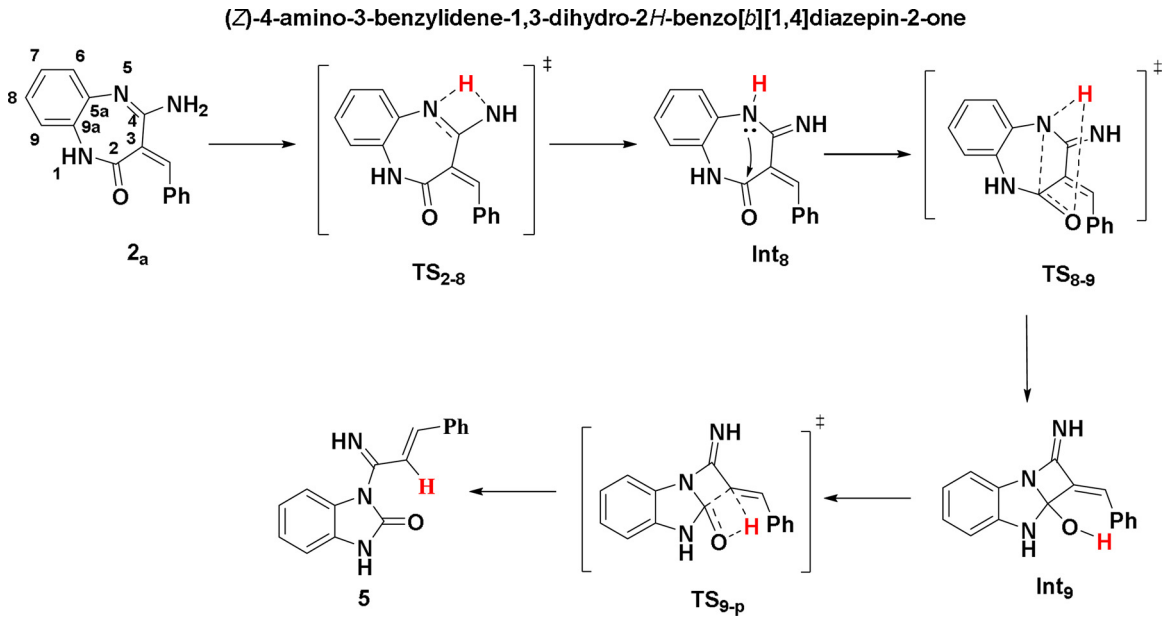


**Scheme 5.** The thermal ring contraction mechanism of 1,5-benzodiazepin-2-one, **2a**, into *N*−alkenylimidazolone derivative **5**.

double bond, where the $C_8$−$C_9$ bond broke as a result of proton transfer to $C_8$ through **$TS_{9\text{-}p}$** four-membered transition state, leading to the scission of the azetidinone ring and furnished the final product, **5**. The depicted free energy profile in Fig. 4 shows that the intramolecular nucleophilic addition in **$Int_8$** is the rate-limiting step along the reaction path with a free energy of 26.70 kcal/mol. Careful analysis of potential energy surface, Fig. 4, showed that the precise transfer of amino hydrogen (red-colored) through $N_1$, $O_1$, and eventually bonded to $C_8$ atom is the play-maker in the reaction game.

## 3. Conclusions and future work

A simple uncatalyzed method was employed to synthesize new members of the 1,5-benzodiazepin-2-ones family (**$2_{a-e}$**) *via* the reaction of α-ethylcyanocinnamate derivatives with *o*-phenylenediamine in xylene. The use of piperidine as a catalyst could successively lead to the formation of *N*−alkenylimidazolone derivative (**5**) in addition to the expected product, 1,5-benzodiazepin-2-one derivative **($2_a$).** Interestingly, **5** was successfully prepared solely by the fusion reaction of 1,5−benzodiazepinones **$2_a$**. Reaction mechanisms were proposed to explain these transformations and have been validated by DFT

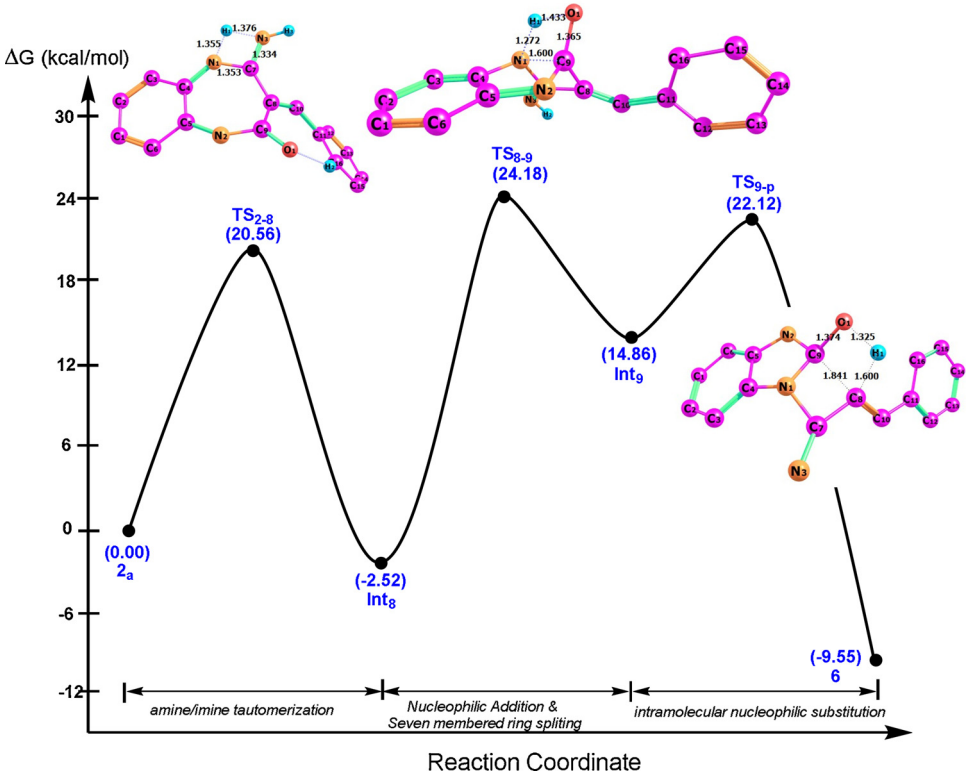


**Fig. 4.** Free energy profile of the thermal ring contraction mechanism of 1,5-benzodiazepin-2-one, $2_a$, into *N*-alkenylimidazolone derivative 5. The optimized structure of transition states is involved in the figure. All hydrogen atoms are omitted for clarity except the interesting ones. (For interpretation of the references to colour in the text, the reader is referred to the web version of this article.)

theoretical analysis. The findings showed the piperidine-catalyzed reaction **$1_a$** + **OPD→5** is more kinetically and thermodynamically favorable than that of **$1_a$** + **OPD →$2_a$** by *ca.* 3 kcal/mol. DFT could successfully explain why **5** was the major product relative to **$2_a$**. We proposed a valid mechanism to account for the formation of **5** *via* the thermal ring contraction of the **$2_a$**. The calculated results are in agreement with the experimental data. Besides, we are going to examine the pharmaceutical properties of the newly synthesized compounds.

## 4. Experimental and computational details

### 4.1. Instrumental measurements

All melting points are uncorrected; they were performed by the open capillary using electrothermal melting MEL_TEMP II apparatus. IR spectra were recorded a UNICAM SP 1200 spectrophotometer using pellet technique KB discs. Micro-analysis was performed in the Faculty of Science, Cairo University, Cairo, Egypt. $^1$H NMR spectra were recorded with Bruker AC spectrometer (200 MHz). $^{13}$C NMR spectra were recorded Bruker AC spectrometer (200 MHz). TMS was used as an internal standard, and chemical shifts are expressed in δ ppm values. The mass spectral data were obtained with micromass spectrometer model 7070F at an energy of 70 eV and inlet temperature 90 °C. All analytical samples were homogenous by thin-layer chromatography, which was performed on EM silica gel 60$F_{254}$ sheet (0.2 mm) the compounds were detected by UV light (254 nm). Ethylcyanoacetate was purchased from Aldrich, and α-ethylcyanocinnamate derivatives (**$1_{a-e}$**) were synthesized as described in the literature using the Knoevenagel procedure [37].

### 4.2. Synthetic methods

#### 4.2.1. 4-Amino-3-arylidine-1,5-benzodiazepin-2-one derivatives ($2_{a-e}$)

*4.2.1.1. General methods*. A mixture of **OPD** (1.08 g, 0.01 mol) and α-cyanocinnamate derivatives **$1_{a-e}$** (0.015 mol) in 40 ml xylene was brought to boil, and the ethanol that formed during the reaction was separated by distillation. Tan crystals began to form according to the reaction mixture, and the mixture was further heated for an additional 6 − 8 h (TLC monitoring). The reaction mixture was cooled, and the product was collected by filtration and crystallized twice from ethanol to give needles crystals of **$2_{a-e}$**.

***4-amino − 3 − phenylidine − 1,5-benzodiazepin-2-one ($2_a$)***: It was obtained as pale gray crystals (50 % yield); M. p. 290 − 291 °C. $^1$H NMR (DMSO − $d_6$): δ = 6.41 − 6.61 [*b*, 4H; N*H*$_2$, N*H* (*exchanged by D$_2$O*), 1H, Ar − *H*]; 7.33 − 7.35 (*t*, 2H, Ar − *H*); 7.59 (*s*, 1H, C − $H_{arom}$.); 7.69 − 7.70 (*m*, 4H, Ar − *H*); 8.27 − 8.29 (*m*, 2H, Ar − *H*). $^{13}$C NMR (100 MHz, DMSO − $d_6$): δ = 151.2, 130.1, 129.7, 128.9, 126.4, 122.0. IR (KBr): ν = 3423(N−H), 3053(C−$H_{arom}$), 2921(C−$H_{aliph}$), 1604(C=C−C=O), 1492(C=N) cm$^{-1}$. Anal. %, Calcd. for $C_{16}H_{13}N_3O$: C, 73.00; H, 4.94; N, 15.96; Found: C, 73.90; H, 5.10; N, 15.10. MS (FD$^+$, THF): *m/z* = 263 [M$^+$].

***4-amino-3-(p-methoxy)phenylidine-1,5-benzodiazepin-2-one ($2_b$)***: It was obtained as yellowish crystals (59 % yield); M. p. 225 − 226 °C. $^1$H NMR (DMSO − $d_6$): δ = 3.94 (*s*, 3H, OC*H*$_3$); 7.20 − 7.32 (*m*, 6H, Ar − *H*, N*H*$_2$, N*H exchanged by D$_2$O*); 7.65 − 7.69 (*m*, 3H; Ar − *H*, C − *H* arom); 8.20 − 8.24 (*d*, 3H, Ar − *H*). $^{13}$C NMR (100 MHz, DMSO − $d_6$): δ = 55.3, 113.8, 114.3, 128.0, 130.1, 151.2, 160.6. IR (KBr): ν = 3426(N−H), 3055(C−$H_{arom}$), 2921(C−$H_{arom}$), 1610(C=C−C=O), 1500(C=N), cm$^{-1}$. Anal. %, Calcd. for $C_{17}H_{15}N_3O_2$, C, 69.62; H, 5.11; N, 14.33; Found: C, 70.10, H, 5.40; N, 13.90. MS (FD$^+$, THF): *m/z* = 295 [M + 2]$^+$.

***4-amino − 3 − (p − chloro)phenylidine − 1,5-benzodiazepin-2-one ($2_c$)***: It was obtained as colorless crystals (51 % yield), m. p. 283 − 284 °C. $^1$H NMR (DMSO − $d_6$): δ = 7.29 − 7.40 (*m*, 3H; N$H_2$, NH *exchanged by D$_2$O*); 7.56 − 7.57 (*d*, 2H, Ar − H); 7.63 − 7.65 (*d*, 2H, Ar − H); 7.69 − 7.71 (*d*, 3H; Ar − H, NH *exchanged by D$_2$O*); 8.21 − 8.23 (*d*, 2H, Ar − H). $^{13}$C NMR (100 MHz, DMSO − $d_6$): δ = 111.4 118.9, 121.7, 122.7, 128.1, 135.0, 143.7, 150.1. IR (KBr): ν = 3447(N−H), 3055(C−$H_{arom}$), 2994(C−$H_{aliph}$), 1605(C=C−C=O), 1477(C=N), cm$^{-1}$. Anal. %, Calcd. for $C_{16}H_{12}N_3OCl$: C, 64.53; H, 4.03; N, 14.11; Found: C, 64.28; H, 3.90; N, 14.10. MS (FD$^+$, THF): *m/z* = 279 [M]$^+$.

***4-amino − 3 − (m − hydroxy)phenylidine − 1,5-benzodiazepin-2-one ($2_d$)***: It was obtained as colorless needles (52 % yield), m. p. 266 °C. IR (KBr): ν = 3400(N−H), 3100(C−$H_{arom}$), 2936(C−$H_{aliph}$), 1584(C=C−C=O), 1466(C=N), cm$^{-1}$. Anal. %, Calcd. for $C_{16}H_{13}N_3O_2$: C, 68.81; H, 4.65; N, 15.05; Found: C, 68.90; H, 4.50; N, 15.68.

***4-amino − 3 − (m − chloro)phenylidine − 1,5-benzodiazepin-2-one ($2_e$)***: It was obtained as colorless crystals (50 % yield), m. p. 220 − 224 °C. $^1$H NMR (DMSO − $d_6$): δ = 7.00 − 7.38 (*m*, 7H; N$H_2$, *exchanged by D$_2$O*, Ar − H, C − H arom.); 7.73 − 7.78 (*m*, 2H, Ar − H); 8.05 − 8.17 (*m*, 3H; Ar − H, NH *exchanged by D$_2$O*). $^{13}$C NMR (100 MHz, DMSO − $d_6$): δ = 111.52, 115.5, 125.0, 126.0, 129.6, 131.0, 132.2, 133.8, 149.7. IR (KBr): 3424(N−H), 3038(C−$H_{arom}$), 2957(C−$H_{aliph}$), 1600(C=C−C=O), 1533(C=N), cm$^{-1}$. Anal. %, Calcd. for $C_{16}H_{12}N_3OCl$: C, 64.53; H, 4.03; N, 14.11; Found: C, 64.40; H, 4.13; N, 14.49.

***4 − amino − 3-dihydro − 1,5 − benzodiazepin(1H) − 2 − one (3)***: A mixture of *o*-phenylendiamine (1.08 g, 0.01 mole) and ethylcyanoacetate (1.59 ml, 0.015 mol) in 40 ml xylene was brought to boil and the water, formed during the reaction, was separated by azeotropic distillation. Faint brown crystals began to separate after 2 h. The reaction mixture was heated for 8 h in the course of which, faint brown crystals formed. The product was collected by filtration and crystallized from ethanol to give needle crystals (70 % yield), m. p. 200 − 205 °C. $^1$H NMR (DMSO-$d_6$): δ = 1.97–2.00 (*m*, 2H, C*H*$_2$); 7.20–7.31 (*m*, 2H, Ar − *H*); 7.57–7.61 (*m*, 2H, Ar − *H*); 7.63–7.64 (*b*, 2H, N*H*$_2$ *exchanged by D$_2$O*); 12.73–12.74 (*b*, 1H, N*H exchanged by D$_2$O*). IR (KBr): ν = 3400(N$H_2$), 3051(C−$H_{arom}$), 2946(C−$H_{aliph}$), 1664(C=O), 1594(C=N) cm$^{-1}$. Anal. %, Calcd. for $C_9H_9N_3O$: C, 61.70; H, 5.18; N, 23.99; Found: C, 61.90; H, 5.00; N, 23.80. MS (FD$^+$, THF): *m/z* = 175 [M]$^+$.

***1-methyl-4-(N-methylamino − 3 − (p − chloro)phenylidine − 1,5-benzodiazepin-2-one (4c)***: A mixture of **$2_c$** (0.01 mole) and sodium ethoxide (0.01 mmol) in absolute ethanol, was stirred at 0 °C. Methyl iodide (0.02 mmol) was added dropwise, and the reaction mixture was stirred for 3 h at room temperature. The resultant crystals were collected, dried, and recrystallized to give 5 in 50 % yield. M. p. 206 °C. $^1$H NMR (DMSO − $d_6$): δ = 8.11–7.98 (*m*, 1H, Ar − *H*); 7.88 − 7.76 (*m*, 3H, Ar − *H*); 7.67 − 7.60 (*m*, 3H, Ar − *H*); 7.20 − 7.16 (*b*, 1H, N*H exchanged by D$_2$O*); 3.87–3.84 (s, 3H, NC*H*$_3$); 3.80–3.75 (*s*, 3H, NC*H*$_3$). $^{13}$C NMR (100 MHz, DMSO-$d_6$): δ = 152.3, 150.8, 142.6, 136.6, 134.7, 131.5 130.4, 130.1, 138.10, 136.0, 127.7, 125.0, 123.3, 122.7, 119.9, 112.9, 109.1, 33.4 (N*C*H$_3$), 31.5 (NC*H*$_3$). IR (KBr): ν = 3350(NH), 3049(C−$H_{arom}$), 2929(C−$H_{aliph}$), 1610(C=O), 1500(C=C) cm$^{-1}$. Anal. %, Calcd. for $C_{18}H_{16}ClN_3O$: C, 66.36; H, 4.95; N, 12.90; Found: C, 66.90; H, 5.00; N, 11.98. MS (FD$^+$, THF): *m/z* = 325 [M]$^+$.

#### 4.2.2. 1-(1-Imino-3-phenylallyl)-1,3-dihydro-2H-benzo[d]imidazol-2-one (5)

*4.2.2.1. Method A*. A mixture of **OPD** (1.08 g, 0.01 mole) and α-cyanocinnamate (**$1_a$**) (0.015 mol) in 50 ml of absolute ethanol and a catalytic amount of piperidine were heated under reflux for 3 h. The reaction mixture was concentrated under reduced pressure, and the products were collected by filtration. Fractional crystallization using ethanol leads to the isolation of two products **$2_a$** and **5** in a 1:3 ratio.

*4.2.2.2. Method B*. 0.02 mol of compounds **$2_a$** in a test tube was plunged in a hot sulfuric bath (~260 °C). The colorless sublimate material which formed above the heated area was repeatedly scraped back into the melt. After 4 h, when sublimation had ceased, the tube

was removed from the bath and allowed to cool, the dark brown solid product was loosened from the wall of the tube by triturating using ethanol (6 ml). The products were collected and crystallized several times from methanol to give brown crystals of **5** (43 % yield); M. p. 273 °C. $^1$H NMR (DMSO − $d_6$): δ = 5.51 (2H, −*HC*═C*H*−), 6.42 (*s*, 1H; Ar − H); 6.49–6.53 (*d*, 1H, Ar − H); 6.65–6.69 (*d*, 1H, Ar − H), 6.95 − 6.99 (*d*, 1H, Ar − H), 7.09 − 7.27 (*m*, 2H, Ar − H), 7.30 − 7.40 (*m*, 2H, Ar − H), 7.73 − 7.76 (*d*, 1H, Ar − H), 9.52 − 9.53 (*b*, 1H, NH *exchanged by $D_2O$*), 9.89 − 9.90 (*b*, 1H, NH *exchanged by $D_2O$*). IR (KBr): $\nu$ = 3338(N−H), 3053(C−$H_{arom}$), 2928 (C−$H_{aliph}$), 1627(C═$O_{amide}$), 1582(C═N) cm$^{-1}$. Anal. %, Calcd. for $C_{16}H_{13}N_3O$: C, 73.00; H, 4.94; N, 15.96; Found: C, 72.90; H, 5.10; N, 16.10. MS (FD$^+$, THF): *m/z* = 263 [M]$^+$.

### 4.3. Computational details

All DFT calculations were performed using a Gaussian 09 software package [41]. B3LYP functional [42,43] with 6-31G(d) basis set were used for geometry optimization. The vibrational frequencies of the optimized stationary points are calculated under the same level of theory, to obtain the zero-point vibrational energy (ZPVE) and thermal corrections at 298 K as well as verifying whether each optimized stationary point is an energy minimum or a transition state. The single-point energies and solvent effects in ethanol were computed with the M06 functional [44,45] based on the gas-phase optimized structures, using 6-311 + G(d,p) basis set for all atoms. The solvation energies were evaluated with the self-consistent reaction field (SCRF) using the SMD implicit solvent model [46].

## CRediT authorship contribution statement

**Hanaa Mansour:** Investigation, Formal analysis, Resources, Data curation, Writing - original draft. **Morad M. El-Hendawy:** Conceptualization, Data curation, Formal analysis, Validation, Investigation, Methodology, Project administration, Visualization, Writing - original draft, Writing - review & editing.

## Declaration of Competing Interest

There are no conflicts to declare.

## Acknowledgment

The authors are thankful to Dr. Mohamed Sadek, Tanta University, Egypt, for his useful discussion.

## Appendix A. Supplementary data

Supplementary material related to this article can be found, in the online version, at doi:https://doi.org/10.1016/j.mcat.2020.110774.

## References

[1] R. Arya, N. Giridharan, V. Anand, S.K. Garg, Cochrane Database Syst. Rev. 7 (7) (2018) CD009258, https://doi.org/10.1002/14651858.CD009258.pub3.
[2] D.A. Horton, G.T. Bourne, M.L. Smythe, Chem. Rev. 103 (2003) 893–930, https://doi.org/10.1021/cr020033s.
[3] Z. Jaafar, S. Chniti, A.B. Sassi, H. Dziri, S. Marque, M. Lecouvey, R. Gharbi, M. Msaddek, J. Mol. Struct. 1195 (2019) 689–701, https://doi.org/10.1016/j.molstruc.2019.06.018.
[4] M. Soyka, N. Engl. J. Med. 376 (2017) 1147–1157, https://doi.org/10.1056/NEJMra1611832.
[5] J.G. Ochoa, W.A. Kilgo, Curr. Treat. Options Neurol. 18 (2016) 1–11, https://doi.org/10.1007/s11940-016-0401-x.
[6] D.J. Hoyle, I.K. Bindoff, L.M. Clinnick, G.M. Peterson, J.L. Westbury, Drugs Aging 35 (2018) 123–134, https://doi.org/10.1007/s40266-018-0518-6.
[7] B.S. Naraboli, J.S. Biradar, Der. Pharma Chem. 9 (2017) 61–69 https://www.derpharmachemica.com/archive/dpc-volume-9-issue-24-year-2017.html.
[8] C.M. Marson, Chem. Soc. Rev. 40 (2011) 5514, https://doi.org/10.1039/c1cs15119c.
[9] P. Cherkupally, S. Ramesh, Y.E. Jad, T. Govender, H.G. Kruger, B.G. de la Torre, F. Albericio, Cyclic peptides as privileged structures, in: S. Bräse (Ed.), Privileged Scaffolds in Medicinal Chemistry: Design, Synthesis, Evaluation, Royal Society of Chemistry, London, 2015, pp. 398–438.
[10] T.N. Ongone, R. Achour, M. El Ghoul, L. El Ouasif, M. El Jemli, L. Chemlal, Y. Cherrah, K. Alaoui, A. Zellou, J. Chem. 2019 (2019) 9043570, , https://doi.org/10.1155/2019/9043570.
[11] H. Salah, E.A. Ahmed, M.M. Hassan, Arab. J. Chem. 10 (4) (2017) 548–555, https://doi.org/10.1016/j.arabjc.2015.03.008.
[12] S. Chander, C.-R. Tang, H.M. Al-Maqtari, J. Jamalis, A. Penta, T.B. Hadda, H.M. Sirat, Y.-T. Zheng, M. Sankarayanan, Bioorg. Chem. 72 (2017) 74–79, https://doi.org/10.1016/j.bioorg.2017.03.013.
[13] H. Mtiraoui, A. Nsira, M. Msaddek, P.Y. Renard, C. Sabot, C. R. Chim. 20 (2017) 747–757, https://doi.org/10.1016/j.crci.2017.02.004.
[14] H. Paghandeh, H. Saeidian, J. Mol. Struct. 1157 (5) (2018) 560–566, https://doi.org/10.1016/j.molstruc.2017.12.035.
[15] M. Hajji, H. Mtiraoui, N. Amiri, M. Msaddek, T. Guerfel, Int. J. Quantum Chem. 119 (2019) 1–13, https://doi.org/10.1002/qua.26000.
[16] T.N. Ongone, R. Achour, M. El Ghoul, L. El Ouasif, K. Taghzouti, M. El Jemli, Y. Cherrah, K. Alaoui, A. Zellou, Adva. Pharm. Sci. 2018 (2018) 6042602, , https://doi.org/10.1155/2018/6042602.
[17] M.V. Sokolovskaya, S.E. Lyubimov, I.S. Mikhel, K.P. Birin, V.A. Davankov, Russ. Chem. Bull. 67 (2) (2018) 260–264, https://doi.org/10.1007/s11172-018-2068-9.
[18] H. Tabata, K. Funaki, T. Tasaka, T. Oshitari, H. Takahashi, H. Natsugari, J. Org. Chem. 84 (24) (2019) 16338–16345, https://doi.org/10.1021/acs.joc.9b02833.
[19] D. Peixoto, A. Locati, C.S. Marques, A. Goth, J.P.P. Ramalho, A.J. Burke, RSC Adv. 5 (121) (2015) 99990–99999, https://doi.org/10.1039/C5RA19599C.
[20] B.M. Reddy, P.M. Sreekanth, Tetrahedron Lett. 44 (2003) 4447–4449, https://doi.org/10.1016/S0040-4039(03)01034-7.
[21] S.R. Sardaa, W.N. Jadhavb, N.B. Kolheb, M.G. Landgec, R.P. Paward, J. Iran. Chem. Soc. 6 (3) (2009) 477–482, https://doi.org/10.1007/BF03246524.
[22] J. Qian, Y. Liu, J. Cui, Z. Xu, J. Org. Chem. 77 (9) (2012) 4484–4490, https://doi.org/10.1021/jo300543n.
[23] J.S. Yadav, B.V.S. Reddy, G. Satheesh, G. Srinivasulu, A.C. Kunwar, Arkivoc 3 (2005) 221–227, https://doi.org/10.3998/ark.5550190.0006.324.
[24] R. Kaoua, N. Bennamane, S. Bakhta, S. Benadji, C. Rabia, B. Nedjar-Kolli, Molecules 16 (1) (2011) 92–99, https://doi.org/10.3390/molecules16010092.
[25] A. Solan, B. Nişanci, M. Belcher, J. Young, C. Schäfer, K.A. Wheeler, B. Török, R. Dembinski, Green Chem. 16 (2014) 1120–1124, https://doi.org/10.1039/C3GC41898G.
[26] G. Saini, P. Kumar, G.S. Kumar, A.R.K. Mangadan, M. Kapur, Org. Lett. 20 (2) (2018) 441–444, https://doi.org/10.1021/acs.orglett.7b03776.
[27] Y. Segawa, T. Maekawa, K. Itami, Angew. Chem. Int. Ed. 54 (2015) 66–81, https://doi.org/10.1002/anie.201403729.
[28] A. Klapars, S. Parris, K.W. Anderson, S.L. Buchwald, J. Am. Chem. Soc. 126 (2004) 3529–3533, https://doi.org/10.1021/ja038565t.
[29] A. Otto, J. Liebscher, Synthesis 8 (2003) 1209–1214, https://doi.org/10.1055/s-2003-39403.
[30] P.M. Kanyonga, M.Y.A. Faouzi, A. Zellou, M.E. Essassi, Y. Cherrah, Int. J. Biol. Chem. Sci. 3 (4) (2009) 646–652 http://ajol.info/index.php/ijbcs.
[31] M. Pérez-Torralba, R.M. Claramunt, M.A. García, C. López, M.C. Torralba, M.R. Torres, I. Alkorta, J. Elguero, Beilstein J. Org. Chem. 9 (2013) 2156–2167, https://doi.org/10.3762/bjoc.9.253.
[32] A. Saber, H. Zouihri, E.M. Essassi, S.W. Ng, Acta Crystallogr. Sect. E: Struct. Rep. Online 66 (pt6) (2010) o1408, https://doi.org/10.1107/S1600536810017885.
[33] Z.-X. Wang, H.-L. Qin, J. Heterocycl. Chem. 42 (5) (2009) 1001–1005, https://doi.org/10.1002/jhet.5570420540.
[34] K. Hitoshi, I. Yuki, I. Tsuneki, Chem. Lett. 35 (12) (2006) 1350–1351, https://doi.org/10.1246/cl.2006.1350.
[35] M. Kawase, H. Koiwai, T. Tanaka, S. Tani, H. Miyamae, Heterocycles 55 (10) (2001) 1919–1926, https://doi.org/10.3987/COM-01-9325.
[36] G. Jones, Org. Reac. 15 (1967) 204–599, https://doi.org/10.1002/0471264180.or015.02.
[37] J.V. Greenhill, Chem. Soc. Rev. 6 (1977) 277–294, https://doi.org/10.1039/CS9770600277.
[38] S. Kumar, K.K. Kapoor, Syn. Lett. 18 (2007) 2809–2814, https://doi.org/10.1055/s-2007-991087.
[39] M. Israel, C. Jones, J. Heterocycl. Chem. 6 (1969) 735–738, https://doi.org/10.1002/jhet.5570060522.
[40] S.I. Okovytyy, L.K. Sviatenko, A.O. Gaponov, I.N. Tarabara, L.I. Kasyan, J. Leszczynski, J. Phys. Chem. A 113 (42) (2009), https://doi.org/10.1021/jp9047709 11376–11342.
[41] M.J. Frisch, G.W. Trucks, H.B. Schlegel, G.E. Scuseria, M.A. Robb, J.R. Cheeseman, G. Scalmani, V. Barone, B. Mennucci, G.A. Petersson, H. Nakatsuji, M. Caricato, X. Li, H.P. Hratchian, A.F. Izmaylov, J. Bloino, G. Zheng, J.L. Sonnenberg, M. Hada, M. Ehara, K. Toyota, R. Fukuda, J. Hasegawa, M. Ishida, T. Nakajima, Y. Honda, O. Kitao, H. Nakai, T. Vreven, J.A. Montgomery, J.E. Peralta, F. Ogliaro, M. Bearpark, J.J. Heyd, E. Brothers, K.N. Kudin, V.N. Staroverov, R. Kobayashi, J. Normand, K. Raghavachari, A. Rendell, J.C. Burant, S.S. Iyengar, J. Tomasi, M. Cossi, N. Rega, N.J. Millam, M. Klene, J.E. Knox, J.B. Cross, V. Bakken, C. Adamo, J. Jaramillo, R. Gomperts, R.E. Stratmann, O. Yazyev, A.J. Austin, R. Cammi, C. Pomelli, J.W. Ochterski, R.L. Martin, K. Morokuma, V.G. Zakrzewski, G.A. Voth, P. Salvador, J.J. Dannenberg, S. Dapprich, A.D. Daniels, Ö. Farkas, J.B. Foresman, J.V. Ortiz, J. Cioslowski, D.J. Fox, Gaussian 09, (2009).
[42] A.D. Becke, J. Chem. Phys. 98 (1993) 5648–5652, https://doi.org/10.1063/1.

464913.
[43] C. Lee, W. Yang, R.G. Parr, Phys. Rev. B 37 (1988) 785–789, https://doi.org/10.1103/PhysRevB.37.785.
[44] Y. Zhao, D.G. Truhlar, Theor. Chem. Acc. 120 (2008) 215–241, https://doi.org/10.1007/s00214-007-0310-x.
[45] Y. Zhao, D.G. Truhlar, Acc. Chem. Res. 41 (2008) 157–167, https://doi.org/10.1021/ar700111a.
[46] A.V. Marenich, C.J. Cramer, D.G. Truhlar, J. Phys. Chem. B 113 (2009) 6378–6396, https://doi.org/10.1021/jp810292n.